Enhancing the european space agency's climate change initiative soil moisture product over China

Wang Y.[a, b, *], Zuo T.[b], Xing F.[b, c], Hu Y.[d], Cui T.[b], Wu J.[e], Shen X.[f, g, h], Wang S.[a] and Xiao Q[a]

[a]Yellow River Institute of Hydraulic Research, Yellow River Conservancy Commission, Zhengzhou, China

[b]College of Geography and Remote Sensing, Hohai University, Nanjing, China

[c]School of Earth Sciences and Engineering, Hohai University, Nanjing, China

[d]Jiangsu Province Hydrology and Water Resources Investigation Bureau, Nanjing, China

[e]College of Hydrology and Water Resources, Hohai University, Nanjing, China

[f]The National Key Laboratory of Water Disaster Prevention, Hohai University, Nanjing, China

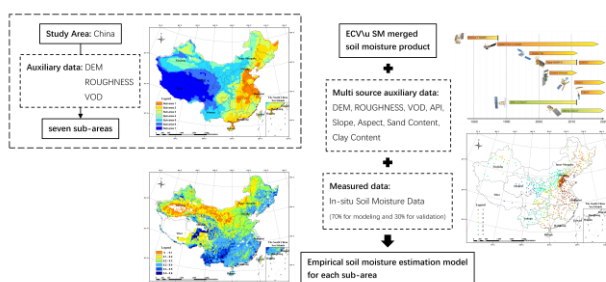[g]Yangtze Institute for Conservation and Development, Hohai University, Nanjing, China

[h]China Meteorological Administration Hydro-Meteorology Key Laboratory, Hohai University, Nanjing, China

Graphical abstract

Abstract

Soil moisture heavily influences the energy exchange between land and the atmosphere, and it plays an important role in ecological systems. Quantitatively acquiring soil moisture information is important for agricultural production, ecological protection and other processes. The current range of soil moisture data products is diverse, but how to enhance the applicability and accuracy of these products in China through data fusion is a question worth exploring. As a new, merged soil moisture product, ECV_SM was initially developed under the European Space Agency's (ESA's) Water Cycle Multi-Mission Observation Strategy (WACMOS) project and is currently being extended and improved within the ESA's Climate Change Initiative (CCI). In this study, an empirical model is suggested to improve the performance of ECV_SM over China. First, the study area was divided into seven sub-areas using digital elevation model (DEM), land surface roughness (ROUGHNESS) and vegetation optical depth (VOD). Then, nine impact factors (DEM, ROUGHNESS, VOD, antecedent precipitation index, slope, aspect, sand content, clay content and ECV_SM) and in-situ soil moisture data were used to build an empirical soil moisture estimation model for each sub-area. In total, 70% of the in-situ soil moisture data was used for modeling and 30% was used for validation. The validation results indicate that the BIAS, root-mean-square difference (RMSD) and mean relative error (MRE) improved from 0.078 cm^3/cm^3 to 0.062 cm^3/cm^3, from 0.099 cm^3/cm^3 to 0.078 cm^3/cm^3, and from 30.0% to 22.6%, respectively. The spatial distribution of the improved dataset is also consistent with the actual conditions. The approach optimizes the ECV_SM product; therefore, the approach is efficient. The results of this study have successfully improved the accuracy of existing data products in China and enhanced the efficiency of data fusion. This has significant implications for the impact of soil moisture products on the regional ecological environment and agricultural production in China.

Keywords: Soil moisture; Essential Climate Variable (ECV); Performance improvement; Partition; Impact factors; Multiple linear stepwise-regression estimation model; China

1. Introduction

Soil moisture plays an extremely important role in ecosystems and agricultural production. The growth and development of plants, their nutrient absorption and transport, and their ability to adapt to environmental changes are all closely related to the conditions of soil moisture. Soil moisture not only affects plant growth but also impacts the activity and diversity of soil microorganisms. These microorganisms play a key role in the nutrient cycling and decomposition of organic matter in the soil, which in turn affects the nutrient supply to vegetation. Appropriate soil moisture is one of the key factors ensuring the healthy growth of crops. Uneven soil moisture can lead to field water management issues, thereby affecting the uniformity and yield of crops. For

Wang Y., Zuo T., Xing F., Hu Y., Cui T., Wu J., Shen X., Wang S. and Xiao Q. (2024), Enhancing the european space agency's climate change initiative soil moisture product over china, *Global NEST Journal*, **26**(6), 05844.

instance, rice requires sufficient waterlogging conditions to thrive, while crops like wheat and soybeans need good drainage to prevent root rot. Accurate monitoring and management of soil moisture can help farmers irrigate more effectively, avoiding over- or under-watering and maximizing the efficiency of water resource use. This can not only increase crop yield but also reduce the wastage of water resources. Utilizing soil moisture sensors, satellite remote sensing technologies, and climate models can help agricultural practitioners better understand and predict soil moisture conditions, thus making more informed decisions. Soil moisture conditions influence subsequent runoff generation, modulate interactions between land surface and atmosphere, and participate in the feedback between land and the atmosphere (McCabe *et al.* 2005). Soil moisture information over a large area would greatly benefit global climate forecasting, drought monitoring and yield estimation.

Microwave remote sensing provides an efficient alternative to quantitatively acquire soil moisture information at various scales. Various microwave instruments have been launched and operated. The types of sensors carried can be roughly divided into two categories: datasets based on active microwave sensors and datasets based on passive microwave sensors. The earliest remote sensing satellites launched with active/passive microwave sensors include SMMR, SMMI, TMI, SCAT, etc. After 2000, remote sensing satellites carrying new active/passive microwave sensors were launched successively, and many soil moisture datasets were generated, such as AMSR-E ((Njoku *et al.* 2003; Owe *et al.* 2008), WindSat ((Li *et al.* 2010; Parinussa *et al.* 2012), Aquarius (Vine *et al.* 2007), ERS-AMI, and MetOp-ASCAT (Bartalis *et al.* 2007; Scipal *et al.* 2002). However, these sensors are not specifically designed for measuring soil moisture, and soil moisture products developed based on these data also differ in design objectives, spatiotemporal resolution and coverage range, data sources, algorithms, and delays (Beck *et al.* 2021). In 2009, the European Space Agency launched an L-band instrument for the Soil Moisture and Marine Salinity (SMOS) mission (Mecklenburg *et al.* 2012). Subsequently, novel and specialized soil moisture datasets such as SMAP (Entekhabi *et al.* 2008) emerged. In 2012, as a follow-up mission to AMSR-E (Parinussa *et al.* 2015), AMSR-2 was launched along with ASCAT sensors based on the MetOp-B platform (Entekhabi *et al.* 2010; Chan *et al.* 2018; O'Neill *et al.* 2019). Between 2014 and 2015, Sentinel-1A and SMAPL (Entekhabi *et al.* 2010; Chan *et al.* 2018; O'Neill *et al.* 2019) were successfully launched. In recent years, new sensors such as radar biomass and NISAR will also be introduced one after another. The development of these instruments has driven the development of (near real-time) soil moisture products, guarantee the continuity of soil moisture products and will contribute to the maturity of microwave remote sensing of soil moisture.

Individual microwave products cannot cover the period required for a climatological or hydrological analysis. Additionally, differences in system and mission designs and the use of different retrieval algorithms have led to data with spatio-temporally varying quality (Dorigo *et al.* 2010; Parinussa *et al.* 2011). Many studies (Karthikeyan *et al.* 2020; Chawla *et al.* 2020; Miralles *et al.* 2019; Tian *et al.* 2019; Brocca *et al.* 2017; Dorigo and Jeu, 2016; Ochsner *et al.* 2013; Albergel *et al.* 2012; Taylor *et al.* 2012; Dorigo *et al.* 2010) have indicated that active and passive microwave data are complementary for different land cover types; radiometers generally perform best over dry areas, while scatterometers perform best over densely vegetated areas (Dorigo *et al.* 2014). Therefore, combining active and passive microwave datasets will contribute substantially to offering improved estimates of surface soil moisture at various scales. In a novel study, Liu *et al.* (2011; 2012;) merged active and passive microwave products into a single multi-decadal ECV for soil moisture (ECV_SM). Subsequently, Dorigo *et al.* (2012) was the first to globally assess trends in the ECV_SM for the period 1988-2010; they compared these trends with soil moisture trends from two model-based surface soil moisture datasets, a precipitation dataset, and a vegetation dataset. Later, Albergel *et al.* (2013) used soil moisture from ERA-Land to monitor the global-scale consistency of ECV_SM and found that ECV_SM is generally relatively stable over time with respect to ERA-Land. Recently, based on existing validation studies, Dorigo *et al.* (2014) provided a more in-depth evaluation of ECV_SM over space and time using ground-based observations. A few years later, their latest research (Dorigo *et al.* 2017) showed that the product quality of ESA CCI SM had steadily increased with each successive release and that the merged products generally outperform the single-sensor input products. However, domestic research over China regarding the ECV_SM product has rarely been conducted.

China is located in eastern Asia on the western Pacific border. China is vast, covering 9.63 million square kilometers. China's average altitude decreases from west to east. The landforms include plateaus, mountains, hills, basins, plains and five basic terrain types. The mountainous area accounts for two-thirds of the surface area. The large latitude range, coupled with the topography, leads to uneven temperature and precipitation distributions. Thus, accurately acquiring soil moisture information for all of China is very difficult when using individual sensor products; many studies (Chen, 2010; Li *et al.* 2013; Xi *et al.* 2014) have demonstrated this point. Chen *et al.* (2012) developed a modified surface roughness index to map the land surface roughness. Combining the microwave polarization difference index (MPDI) and the modified surface roughness index, they derived a semi-empirical model for soil moisture. The model was validated using in situ observations, indicating the effectiveness of the model, although it was only examined in Guangdong Province, southern China. The aforementioned studies primarily focused on validation and algorithm development for soil moisture in China. Some scientists have concentrated on improving the performance of the existing remote sensing soil moisture datasets over China. Yan *et al.* (2008) constructed multiple

linear estimation models for Yanan City, China, with backward and forward stepwise regression. Ma (2007) improved the retrieval algorithm for AMSR-E soil moisture data over Xinjiang Province, China, using MPDI and calculated the vegetation opacity. The average correlation coefficient between the improved dataset and the ground-based dataset was found to be 0.811.

The new and synthetic soil moisture product, ECV_SM, will provide new research opportunities for studying soil moisture and climate patterns in China. Therefore, this study aims to establish a multiple stepwise linear-regression model for the ECV_SM product using in-situ soil moisture data over China and to improve the data accuracy over China. Additionally, the improved ECV_SM product is validated to show the good performance of the improvement method.

2. Materials and methods

2.1. The ECV_SM dataset

ECV_SM (Version 02.0) is a newly merged soil moisture product developed under the framework of the European Space Agency's Water Cycle Multi-mission Observation Strategy (WACMOS) and CCI projects. The product was generated by spaceborne active and passive microwave instruments; it originates from a number of Earth Observation (EO) missions, agencies and sensor systems. The active dataset was generated by the University of Vienna using observations from the C-band scatterometers on board ERS-1/2 and METOP-A. The passive dataset was generated by the VU University Amsterdam in collaboration with NASA using passive microwave observations from Nimbus 7 SMMR, DMSP SSM/I, TRMM TMI, Aqua AMSR-E, Coriolis WindSat, and GCOM-W1 AMSR2. As shown in Figure 1, the suite of datasets covers a 35-year period, from the late 1970s to the present. At present, the product provides global coverage at a spatial resolution of 0.25 degrees.
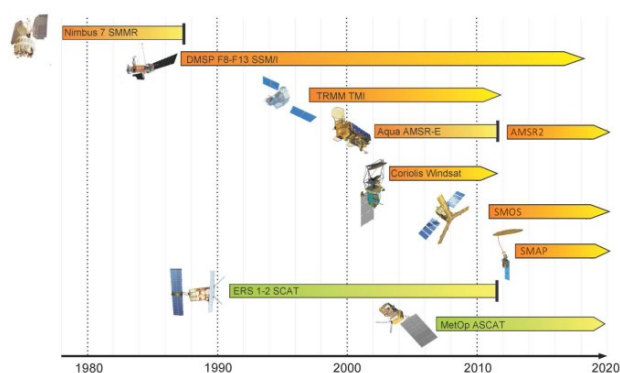
Figure 1. An overview of the active and passive sensors that provide the ECV_SM product (source: WACMOS project (2012))

2.2. Ground-based data

A standard ground-based dataset, named CHINA, was obtained from the International Soil Moisture Network (ISMN) and was produced by the Institute of Geographic Sciences and Natural Resources Research of the Chinese Academy of Sciences. A total of 40 stations are mainly distributed throughout northeastern and eastern China.

The in-situ soil moisture data, which are derived from the Chinese crop growth and farmland soil moisture dataset, were downloaded from the China Meteorological Data Sharing Service System.

2.3. Auxiliary datasets

The brightness temperature dataset from the AMSR-E Level-3 land surface product (AE_Land3) was downloaded from the American National Snow and Ice Data Center. The data with a 56-km mean spatial resolution are resampled to global cylindrical 25-km Equal-Area Scalable Earth Grid (EASE-Grid) cell spacing. The data are stored in HDF-EOS format and are available via FTP.

AMSR2 (Advanced Microwave Scanning Radiometer 2) is an improved version of AMSR (Aperture 2.0 meters) on ADEOS II and AMSR-E (Aperture 1.6 meters) on NASA Aqua satellites. AMSR-2 is onboard GCOM-W1, which was developed by the Japan Aerospace Exploration Agency (JAXA) and launched successfully on 18 May 2012. AMSR-2 is a passive microwave remote sensing instrument that cannot emit electromagnetic waves but can detect the characteristics of a target by passively receiving the microwave energy emitted by the observed object. AMSR-2 is a seven-frequency passive microwave radiometer system that measures brightness temperatures at 6.9, 7.3, 10.7, 18.7, 23.8, 36.5, and 89.0 GHz in horizontal and vertical polarization modes, resulting in a total of 14 observation channels. Each scanning band contains data from the relevant scanning area, which are stored in HDF5, a hierarchical data format with L1R representing the resampled data (Shen *et al*. 2019).

The soil dataset of China, which is from the Harmonized World Soil Database (HWSD), was downloaded from the Heihe Plan Science Data Center of the National Natural Science Foundation of China. The dataset includes the following attributes: soil name, classification, soil texture, soil depth, soil water content, sand content, and silt content. The data are gridded using the WGS-84 projection.

The land cover products for China were downloaded from the Cold and Arid Regions Science Data Center. In these products, China's land surface is divided into 17 categories, including evergreen broadleaf forests, grasslands, permanent wetlands, croplands, urban and built-up lands, glaciers and water bodies (Ran *et al.* 2006; Ran *et al.* 2012).

The daily gridded precipitation data are extracted from the real-time rainfall data at more than 2400 sites and are downloaded from the China Meteorological Data Sharing Service System.

2.4. Data preprocessing

In-situ soil moisture data were collected from agrometeorological stations on the eighth day of every ten-day interval each month. A maximum merging method was used to process ECV_SM and to unify the time periods of the two datasets. The ECV_SM data observed on the 7th, 8th and 9th day of every month were merged. A similar procedure was performed on the 17th,

18th and 19th days and on the 27th, 28th and 29th days. This procedure not only retains the temporal characteristics of the soil moisture data but also eliminates noise in the observations. Pixel values in the ice-covered and densely vegetated regions, where the microwave band was not viable, were rejected. A 5-by-5 moving window was used to inspect every pixel and fill the rejected pixels with the average of nearby values.

The selection of suitable stations for the soil moisture data was based on the criteria in the Product Validation Plan. A total of 533 stations were obtained. The field capacity was calculated using the China soil dataset. This procedure was used to convert in-situ soil moisture data into volumetric water content (cm^3/cm^3). The in-situ soil moisture data were evaluated using the standard CHINA dataset. The results show that the two datasets are significantly similar. The average correlation coefficient is 0.811, which passed the significance test at $p=0.005$. Thus, the in-situ soil moisture data were used in the modeling and validation procedures.

2.5. Model parameter analysis and acquisition

The effects of vegetation cover and vegetation water content on soil moisture are manifested as the water interception effect of crowns, the reduction of soil water evaporation and the increase in transpiration losses. Litter cover and plant roots can enhance soil water infiltration, which impacts soil moisture (Qiu *et al.* 2007). The effects of meteorological factors on soil moisture are mainly reflected in the precipitation. Hawley *et al*. (1983) and Henninger *et al*. (1976) found that the spatial variability and average value of soil moisture varies with precipitation changes and that consistent trends in seasonal variations occur. The main terrain factors are the slope, aspect and elevation. Generally, soil moisture decreases as the slope increases. The influence of the aspect on soil moisture is mainly manifested as a difference in solar radiation. Soil water preservation is mainly determined by the soil porosity and soil texture: a smaller soil particle size corresponds to increased preservation (Owe *et al.* 2001; Parinussa *et al.* 2011). Therefore, the following nine factors were used to build the empirical soil moisture model: DEM, ROUGHNESS, VOD, API, slope, aspect, SAND, CLAY and ECV_SM.

2.6. Retrieving the API

The following API definition, which was proposed in the 1950s by Kohler and Linsley (McQuigg, 1954), was applied in this study:

$$API(i)=P(i)+kAPI(i-1) \qquad (1)$$

where P is the precipitation and k is the attenuation coefficient of the API.

Equation (1) can be expanded as follows:

$$API(i)=\sum_{d=0}^{\infty}k^d \cdot P(i-d) \qquad (2)$$

In this study, k was set to 0.9 based on previous studies (Jr., 2002; Yuan and Zhou, 2004), and the influence of the

two prior months was considered when calculating the API.

2.7. Retrieving roughness

According to microwave radiation transfer theory, surface soil moisture, VOD and canopy temperature greatly influence canopy brightness temperatures. In the Jin (1998) surface-roughness empirical model, the rough surface reflectivity is represented as

$$r_{sv}=\left[\left(1-Q\right)r_{ov}+Qr_{oh}\right]e^{-h} \qquad (3)$$

$$r_{sh}=\left[\left(1-Q\right)r_{oh}+Qr_{ov}\right]e^{-h} \qquad (4)$$

where Q is a polarization mixing parameter, which ranges between 0 and 0.5; h is the vertical surface roughness parameter; r_{sv} and r_{sh} represent the vertical and horizontal polarization reflectivities, respectively, of a rough surface; and r_{ov} and r_{oh} represent the vertical and horizontal polarization reflectivities, respectively, of a flat surface.

Therefore, the MPDI can be characterized as follows (Ma, 2007):

$$\frac{1}{MPDI}=\frac{r_{ov}+r_{oh}}{\left(1-2Q\right)\left(r_{ov}-r_{oh}\right)}-\frac{1}{\left(1-2Q\right)\left(r_{ov}-r_{oh}\right)}2e^{2\tau_c+h} \qquad (5)$$

where $r_{ov}+r_{oh}$ and $(1-2Q)(r_{ov}+r_{oh})$ are only affected by soil moisture. Three MPDIs can be obtained from AMSR-E 6.9 GHz, 10.7 GHz and 18.7 GHz brightness temperature data to calculate Γ (Ma, 2007):

$$\Gamma=\frac{\dfrac{1}{MPDI_{6.9}}-\dfrac{1}{MPDI_{10.7}}}{\dfrac{1}{MPDI_{18.7}}-\dfrac{1}{MPDI_{10.7}}}=\frac{e_{6.9}^{2\tau_c+h}-e_{10.7}^{2\tau_c+h}}{e_{18.7}^{2\tau_c+h}-e_{10.7}^{2\tau_c+h}} \qquad (6)$$

Here, Γ is affected not only by the surface roughness but also by the vegetation coverage; consequently, Γ cannot represent ROUGHNESS well. Chen (2012) assumed that a linear relation exists among the various AMSR-E bands, namely, $e_{6.9}^{\tau_c} \approx me_{10.7}^{\tau_c} \approx ne_{18.7}^{\tau_c}$, where m and n are coefficients. Thus, the following equation is derived (Chen *et al.* 2012):

$$\frac{\dfrac{1}{MPDI_{6.9}}-\dfrac{1}{MPDI_{10.7}}}{\left(\dfrac{1}{MPDI_{18.7}}-\dfrac{1}{MPDI_{10.7}}\right)e_{6.9}^{2\tau_c}}=\frac{1-m}{n-m}*\frac{e_{6.9}^h-e_{10.7}^h}{e_{18.7}^h-e_{10.7}^h} \qquad (7)$$

Using Owe's vegetation optical depth (Owe *et al.* 2001), a simple surface roughness index (Γ_{MPDI}) can be characterized (in cm) as follows (Chen *et al.* 2012):

$$\Gamma_{MPDI} \approx -3.21111\times\frac{\dfrac{1}{MPDI_{6.9}}-\dfrac{1}{MPDI_{10.7}}}{\left(\dfrac{1}{MPDI_{18.7}}-\dfrac{1}{MPDI_{10.7}}\right)} \qquad (8)$$

$$\times\left(MPDI_{6.9}-0.33280\right)+0.00178$$

Here, Γ_{MPDI} is only influenced by the surface roughness of h; hence, Γ_{MPDI} more reasonably represents ROUGHNESS than does Γ. Subsequently, Chen (2012) verified the results of using Γ_{MPDI} and demonstrated its high accuracy. In this study, the ROUGHNESS was retrieved using the above method.

3. Results and discussion

3.1. Partitioning and modeling

The vastness of China has a profound effect on the spatial variation in soil moisture; therefore, the area must be partitioned. Soil moisture is closely related to topography, geomorphology, vegetation, and other factors. Among the data used, DEM data can accurately reflect the topographical conditions, the roughness factor can accurately reflect the geomorphological conditions, and VOD data can represent the impact of vegetation factors on soil moisture. Each factor affects the soil moisture modeling: DEM influences through elevation and slope, ROUGHNESS through the land surface texture, and VOD as a measure of vegetation density, which impacts soil moisture through transpiration and interception. The study area was divided into seven sub-areas using DEM, ROUGHNESS and VOD, as shown in Figure 2.
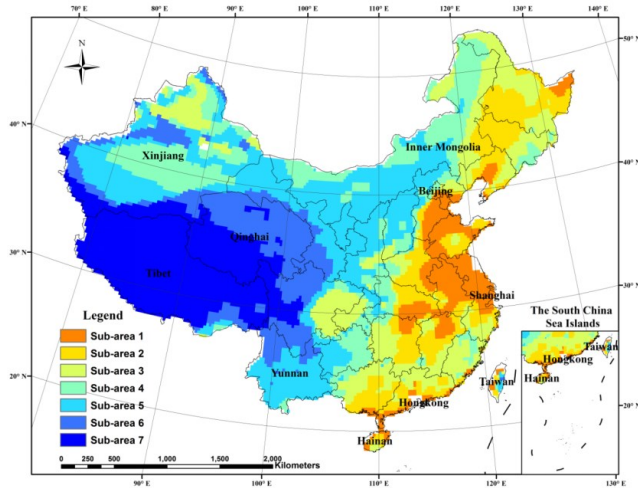
Figure 2. The partitioning result for China using an unsupervised classification

Surface soil moisture modeling relies on many factors; thus, the precision of ECV_SM can be improved by establishing a regression model. The model can be characterized as follows:

$$SM = a_1 X_1 + a_2 X_2 + a_3 X_3 + \cdots a_n X_n \qquad (9)$$

where SM is the surface soil moisture; X_1, X_2, X_3, X_n are various factors that influence SM; a_1, a_2, a_3, $\ldots$ a_n are coefficients of the multiple regression calculation; and n is the number of impact factors.
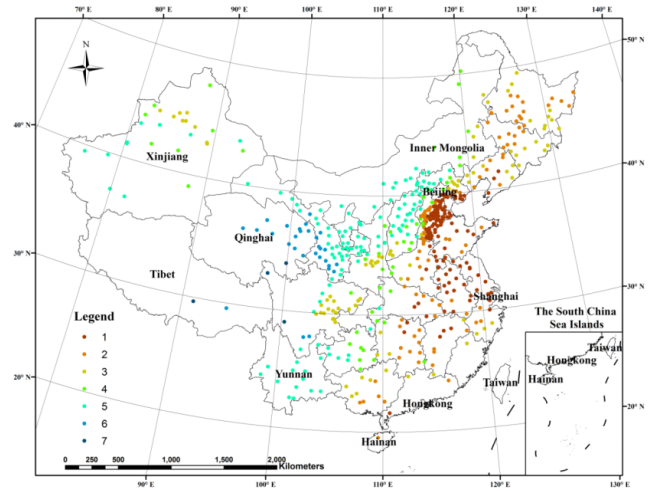
Figure 3. The distribution of the agrometeorological stations in each sub-area

Many factors were considered when establishing the multiple linear stepwise-regression model; however, the parameter dimensions were not consistent. Therefore, normalization was applied when processing the datasets to eliminate the influence of the different parameter dimensions. The agrometeorological station soil moisture data were preprocessed and classified based on the seven sub-areas (Figure 3). To evaluate the precision of the modeling results, the data of each sub-area were divided into two parts: 70% of the data was used for modeling and the other 30% was used for validation. Because the nine selected parameters differently affect the soil moisture within each sub-area, a backward method was used to construct a multiple linear-regression model for China for 2020 (specifically, early October).

3.2. Validation and Analysis

The parameter selection results in each sub-area are shown in Table 1. Lack of the observational data for the seventh sub-area led to the failure of the modeling process.

Table 1. An overview of the selected factors for simulating each sub-area

Elements	Partition						Number of occurrences
	1	2	3	4	5	6	
API		√	√	√	√	√	5
ASPECT				√	√	√	3
ECV_SM	√		√		√		3
CLAY			√	√			2
DEM					√		1
ROUGHNESS					√		1
SAND	√	√	√		√	√	5
SLOPE	√			√	√	√	4
VOD				√			1

Table 2. Multiple linear regression models for each sub-area

Partition	Station Number for Modeling	Model	R	Adjust R^2	p
1	80	SM = 0.396*CCI-0.156*SAND+0.230 *SLOPE+0.233	0.543	0.266	0.000
2	65	SM = 0.078*API-0.396*SAND+0.477	0.579	0.313	0.000
3	57	SM = -0.206*SAND+0.155*API+0.313*CCI-0.130 *CLAY+0.370	0.735	0.505	0.000
4	28	SM = 0.310*API+0.077*ASPECT+0.25 *CLAY+0.146*SLOPE-0.104	0.746	0.473	0.001
5	72	SM = 0.286*API+0.029*ASPECT+0.040 *CCI-0.149*DEM+0.095 *ROUGHNESS-0.232*SAND+0.029 *SLOPE+0.022*VOD+0.231	0.802	0.596	0.000
6	13	SM = 0.150*API-0.311*ASPECT+0.2 *SAND -0.148 *SLOPE+0.343	0.854	0.594	0.021

Table 3. Validation results

Partition	Validation Station Number	Original Data					Improved Data				
		BIAS (cm^3/cm^3)	RMSD	MRE	R^2	p-value	BIAS	RMSD	MRE	R^2	p-value
1	35	0.075	0.096	0.299	0.380	0.000	0.062	0.076	0.222	0.372	0.000
2	28	0.078	0.105	0.270	0.296	0.004	0.073	0.095	0.234	0.251	0.010
3	25	0.081	0.097	0.318	0.246	0.013	0.043	0.056	0.221	0.433	0.000
4	12	0.080	0.109	0.426	0.126	0.283	0.071	0.083	0.359	0.413	0.024
5	31	0.079	0.096	0.285	0.301	0.001	0.062	0.078	0.265	0.430	0.000
6	6	0.080	0.085	0.271	-	-	0.049	0.058	0.185	-	-
Average		0.078	0.099	0.300	0.270	-	0.062	0.078	0.226	0.380	-

Based on Table 1, the API and SAND appear five times; thus, these two factors most greatly affect soil moisture. The ECV_SM product appears three times, which could be attributed to the limitations of the microwave dataset, particularly in the high-altitude area (>800 m) where the precision is low. Notably, VOD, ROUGHNESS and DEM were found to be important factors that affected soil moisture in our previous analysis, but the model participation rates were not high. The three factors used for the partitioning process exhibit similar performances within the same sub-area; therefore, these factors are not considered important in the soil moisture modeling.

R is the multiple correlation coefficient of the regression model; this coefficient represents the linear relationship between an independent variable and dependent variable. Compared with R^2, the adjusted R^2 can better suppress the influence of variable numbers and sample sizes. p is the significance. Based on Table 2, the significance of the models in sub-areas 1, 2, 3 and 5 are very good compared with those in sub-areas 4 and 6 because of the abundant in-situ data. All models passed the 95% significance level test. Table 3 shows the results of the validation models using the remaining 30% of the data.

Based on Table 3, all statistical measures pertaining to each sub-area improved after the simulations. The improvements in sub-areas 3 and 6 are particularly notable; however, the amount of observational data for sub-area 6 is small, leading to uncertainty in the results. Generally, the models performed well; thus, the improved ECV_SM can be used for soil moisture related studies and applications. Figure 4 shows the China soil moisture

distribution map. Null pixel information is displayed in white due to the lack of values in the original ECV_SM product, and the seventh sub-area relied on the original ECV_SM data because of the failure of the modeling process.
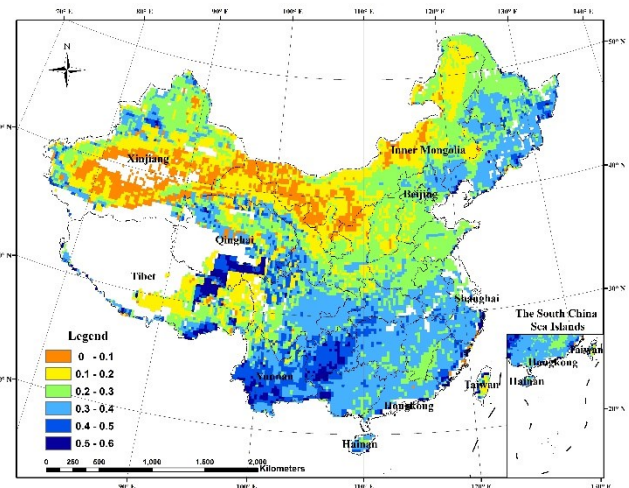

Figure 4. China soil moisture map derived from the improved ECV_SM in early October 2020 (cm^3/cm^3)

Figure 4 presents an overview of the spatial distribution of the surface soil moisture according to the improved ECV_SM product. Overall, the northwest is dry, and the southeast is wet. A high soil moisture value between 0.3 cm^3/cm^3 and 0.5 cm^3/cm^3 is mainly found south of the Qinling Mountains to the Huaihe River, the three northeastern provinces and the eastern Tibetan Plateau. This finding is consistent with the geographical

distribution of the humid areas. The abnormally high soil moisture value in the southern Tibetan Plateau is attributed to the original ECV_SM data. A low soil moisture value between 0 and 0.1 is mainly observed in Xinjiang province and central Inner Mongolia province. This finding is consistent with the actual conditions of arid areas. A soil moisture value between 0.1 and 0.3 is mainly observed near the dry-wet climate boundary. A soil moisture value between 0.1 and 0.2 is observed in the Inner Mongolia Plateau, Central Xinjiang, the Tibetan Plateau and the Loess Plateau. The regions whose soil moisture value ranges from 0.2 to 0.3 are located in the North China Plain, the Northeast China Plain, the Loess Plateau and northern Xinjiang province. From the above analysis, we found that the ECV_SM optimization results are similar to the spatial patterns of drought and wet soil in China and therefore reflect the rationality of the research. In addition, the average soil moisture contents of Yunnan and Guizhou are the highest among all of the provinces because rainfall occurred in early October in these areas. The abnormally high soil moisture contents in the northeastern Tibetan Plateau may be caused by the insufficient in situ observational data.

4. Conclusions and recommendations

In this research, the study area was initially divided into seven sub-areas using DEM, ROUGHNESS and VOD. The VOD, API, DEM, SLOPE, ASPECT, SAND, CLAY, ROUGHNESS and ECV_SM parameters, which greatly influence the soil moisture, were selected to build the empirical soil moisture multiple stepwise-regression model; 70% of the in-situ soil moisture observations was applied to modeling, and the remaining 30% of the data was used to validate the accuracy. The soil moisture map of China for 2020 (early October) was consistent with the actual conditions. The validation results show that the BIAS, RMSD and MRE were improved from 0.078 cm^3/cm^3 to 0.062 cm^3/cm^3, from 0.099 cm^3/cm^3 to 0.078 cm^3/cm^3 and from 30.0% to 22.6%, respectively. The approach optimizes the ECV_SM product; therefore, the method is efficient. However, the approach only filled the sporadic null pixel values in the study area, and a large unfilled district remained unprocessed. In addition, because of the influence of ice-covered soil and low temperatures, a large number of agrometeorological stations lack measured data from winter. This data scarcity has an impact on the calibration results. Furthermore, the research is limited to short-term data. In future studies, this problem, as well as the identification of the partitioning and modeling rules, will be considered to generate new methods of evaluating large areas and multiple temporal and high-precision soil moisture data sets. Additionally, future studies will consider the use of more advanced soil moisture sensing technologies or methods to improve the accuracy of research data. Furthermore, efforts will be made to enhance the applicability and improvement methodologies of specific data in extreme areas such as high-altitude regions, providing more comprehensive data outcomes for the research.

References

(2012) Data Access Requirements Document, ESA.

Albergel C., de Rosnay P., Gruhier C., Munoz-Sabater J., Hasenauer S., Isaksen L., Kerr Y. and Wagner W. (2012). Evaluation of remotely sensed and modelled soil moisture products using global ground-based in situ observations. *Remote Sensing of Environment* **118**, 215-226.

Albergel C., Dorigo W., Balsamo G., Muñoz-Sabater J., de Rosnay P.d., Isaksen L., Brocca L., de Jeu R. and Wagner W. (2013). Monitoring multi-decadal satellite earth observation of soil moisture products through land surface reanalyses. *Remote Sensing of Environment* **138**.

Baldwin D., Manfreda S., Lin H., and Smithwick E.A.H. (2019). Estimating root zone soil moisture across the eastern united states with passive microwave satellite data and a simple hydrologic model. *Remote Sensing*, **11**(17), 2013.

Bartalis Z., Wagner W., Naeimi V., Hasenauer S., Scipal K., Bonekamp H., Figa J. and Anderson C. (2007). Initial soil moisture retrievals from the METOP-A Advanced Scatterometer (ASCAT). *Geophysical Research Letters* **34**(20).

Beck H.E., Pan M., Miralles D.G., Reichle R.H. and Wood E.F. (2021). Evaluation of 18 satellite- and model-based soil moisture products using in situ measurements from 826 sensors. *Hydrology and Earth System Sciences*, **25**(1), 17–40.

Blyverket J., Hamer P.D., Bertino L., Clément Albergel and Lahoz W.A. (2019). An evaluation of the enkf vs. enoi and the assimilation of smap, smos and esa cci soil moisture data over the contiguous us. *Remote Sensing*, **11**(5).

Brocca L., Crow W.T., Ciabatta L., Massari C., de Rosnay P., Enenkel M., Hahn S., Amarnath G., Camici S., Tarpanelli A. and Wagner W. (2017). A review of the applications of ASCAT soil moisture products, *IEEE Journal of Selected Topics in Applied*., **10**, 2285–2306.

Chan S.K., Bindlish R., O'Neill P., Jackson T., Njoku E., Dunbar S., Chaubell J., Piepmeier J., Yueh S., Entekhabi D., Colliander A., Chen F., Cosh M.H., Caldwell T., Walker J., Berg A., McNairn H., Thibeault M., Martinez-Fernández J., Uldall F., Seyfried M., Bosch D., Starks P., Holifield Collins C., Prueger J., van der Velde R., Asanuma J., Palecki M., Small E.E., Zreda M., Calvet J., Crow W.T. and Kerr Y. (2018). Development and assessment of the SMAP enhanced passive soil moisture product, *Remote Sensing of Environment*., **204**, 931–941.

Chawla I., Karthikeyan L. and Mishra A.K. (2020). A review of remote sensing applications for water security: quantity, quality, and extremes, *Journal of Hydrology*., **585**, 124826.

Chen J. (2010). Validation of AMSR-E soil moisture products in northwest of China. M.S. thesis, Chinese Academy of Meteorological Sciences, Beijing, China.

Chen X.Z., Chen S.S., Zhong R.F., Su Y.X., Liao J.S., Li D., Han L.S., Li Y. and Li X. (2012). A semi-empirical inversion model for

assessing surface soil moisture using AMSR-E brightness temperatures. *Journal of Hydrology* **456**, 1–11.

Dorigo W. and de Jeu R. (2016). Satellite soil moisture for advancing our understanding of earth system processes and climate change, *international Journal of Applied Earth Observation*, **48**, 1–4.

Dorigo W., Jeu R.d., Chung D., Parinussa R., Liu Y., Wagner W. and Fernández-Prieto D. (2012). Evaluating global trends (1988-2010) in harmonized multi-satellite surface soil moisture. *Geophysical Research Letters* **39**(18).

Dorigo W.A., Gruber A., De Jeu R.A.M., Wagner W., Stacke T., Loew A., Albergel C., Brocca L., Chung D., Parinussa R.M. and KiddR. (2014). Evaluation of the ESA CCI soil moisture product using ground-based observations. *Remote Sensing of Environment* (**0**).

Dorigo W.A., Scipal K., Parinussa R.M., Liu Y.Y., Wagner W., de Jeu R.A.M. and Naeimi V. (2010). Error characterisation of global active and passive microwave soil moisture datasets. *Hydrology and Earth System Sciences* **14**(12), 2605–2616.

Entekhabi D., Njoku E., O'Neill P. and Spencer M. (2008). The Soil Moisture Active/Passive Mission (SMAP), pp. III - 1 - III - 4.

Entekhabi D., Njoku E.G., O'Neill P.E., Kellogg K.H., Crow W.T., Edelstein W.N., Entin J.K., Goodman S.D., Jackson T.J., Johnson J., Kimball J., Piepmeier J.R., Koster R.D., Martin N., McDonald K.C., Moghaddam M., Moran S., Reichle R., Shi J.C., Spencer M.W., Thurman S.W., Tsang L. and Van Zyl J. (2010). The Soil Moisture Active Passive (SMAP) mission, P. IEEE, **98**, 704–716.

Gao H., Wood E.F., Jackson T.J., Drusch M. and Bindlish R. (2006). Using TRMM/TMI to Retrieve Surface Soil Moisture over the Southern United States from 1998 to 2002. *Journal of Hydrometeorology*. **7**, 23.

Hawley M.E., Jackson T.J. and McCuen R.H. (1983). Surface soil moisture variation on small agricultural watersheds. Journal of Hydrology **62**(1–4), 179–200.

Henninger D.L., Petersen G.W. and Engman E.T. (1976). Surface Soil Moisture within a Watershed Variations, Factors Influencing, and Relationship to Surface Runoff. *Soil Science Society of America Journal* **5**, 773–776.

Jin Y.Q. (1998). Monitoring regional sea ice of China's Bohai Sea by SSM/I scattering indexes. Ieee J Oceanic Eng **23**(2), 141–144.

Jr. R.R.H. (2002). A review of twentieth-century drought indices used in the United States. Bull. Amer. Meteorol. Soc. **83**, 1149–1165.

Karthikeyan L., Chawla I. and Mishra A.K. (2020). A review of remote sensing applications in agriculture for food security: crop growth and yield, irrigation, and crop losses, *Journal of Hydrometeorology*., 124905.

Li A., Lu Q.F., Yang X.F. and Zhang J.W. (2013). AMSR-E Soil Moisture Compared with ECWMF and NECP Soil Moisture. *Remote Sensing Technology and Application* **28**(4), 666–673.

Li L., Gaiser P.W., Gao B.C., Bevilacqua R.M., Jackson T.J., Njoku E.G., Rudiger C., Calvet J.C. and Bindlish R. (2010). WindSat Global Soil Moisture Retrieval and Validation. *Ieee Transactions on Geoscience and Remote Sensing* **48**(5), 2224–2241.

Liu Y.Y., Dorigo W.A., Parinussa R.M., de Jeu R.A.M., Wagner W., McCabe M.F., Evans J.P. and van Dijk A.I.J.M. (2012). Trend-preserving blending of passive and active microwave soil

moisture retrievals. *Remote Sensing of Environment* **123**, 280–297.

Liu Y.Y., Parinussa R.M., Dorigo W.A., de Jeu R.A.M., Wagner W., van Dijk A.I.J.M., McCabe M.F. and Evans J.P. (2011). Developing an improved soil moisture dataset by blending passive and active microwave satellite-based retrievals. *Hydrology and Earth System Sciences* **15**(2), 425–436.

Ma Y. (2007) Study on Soil Moisture Inversion and Application with Microwave Remote Sensing in Xinjiang., Xinjiang University.

McCabe M.F., Gao H. and Wood E.F. (2005). Evaluation of AMSR-E-derived soil moisture retrievals using ground-based and PSR airborne data during SMEX02. J. Hydrometeorol. **6**(6), 864–877.

McQuigg J. (1954). A simple index of drought conditions. Weatherwise, 64–67.

Mecklenburg S., Drusch M., Kerr Y.H. and Font J. (2012). ESA's Soil Moisture and Ocean Salinity Mission: Mission Performance and Operations. Geoscience and Remote Sensing, *IEEE Transactions on* **50**(5), 1354–1366.

Miralles D.G., Gentine P., Seneviratne S.I. and Teuling A.J. (2019). Land-atmospheric feedbacks during droughts and heatwaves: state of the science and current challenges, *Annals of the New York Academy of Sciences.*, 1436, 19–35.

Njoku E.G., Jackson T.J., Lakshmi V., Chan T.K. and Nghiem S.V. (2003). Soil moisture retrieval from AMSR-E. *IEEE Transactions on Geoscience and Remote Sensing* **41**(2), 215–229.

Ochsner T.E., Cosh M.H., Cuenca R.H., Dorigo W.A., Draper C.S., Hagimoto Y., Kerr Y.H., Larson K.M., Njoku E.G., Small E.E., and Zreda M. (2013). State of the art in large-scale soil moisture monitoring, *Soil Science Society of America Journal.*, **77**, 1888–1919.

O'Neill P.E., Chan S., Njoku E.G., Jackson T. and Bindlish R. (2019). SMAP Enhanced L3 radiometer global daily 9km EASEgrid soil moisture, version 3, National Snow and Ice Data Center, Boulder, USA.

Owe M., de Jeu R. and Walker J. (2001). A methodology for surface soil moisture and vegetation optical depth retrieval using the microwave polarization difference index. *Ieee Transactions on Geoscience and Remote Sensing* **39**(8), 1643–1654.

Owe M., Jeu R.d. and Holmes T. (2008). Multisensor historical climatology of satellite-derived global land surface moisture. *Journal of Geophysical Research: Earth Surface* (2003–2012) 113(F1).

Parinussa R., Meesters A.G.C.A., Liu Y.Y., Dorigo W., Wagner W. and De Jeu R.A.M. (2011). An analytical solution to estimate the error structure of a global soil moisture data set. *IEEE Geoscience and Remote Sensing Letters* **8**, 779–783.

Parinussa R.M., Holmes T.R.H., Wanders N., Dorigo W.A. and de Jeu R.A.M. (2015). A preliminary study toward consistent soil moisture from AMSR2, *Journal of Hydrometeorology.*, **16**, 932–947.

Parinussa R.M., Holmes T.R.H. and Jeu R.A.M.d. (2012). Soil Moisture Retrievals From the WindSat Spaceborne Polarimetric Microwave Radiometer. *IEEE T. Geoscience and Remote Sensing* **50**.

Qiu Y., Fu B., Wang J., Zhang X. and Meng Q. (2007). Spatio temporal variation of soil moisture and its relation to

environmental factors. *Chinese Journal of Ecology* **26**(1), 100–107.

Ran Y.H., Li X. and Lu L. (2006). China Land Cover Classification at 1km Spatial Resolution Based on a Multi-source Data Fusion Approach. *ADVANCES IN EARTH SCIENCE* **24**(2), 192–203.

Ran Y.H., Li X., Lu L. and Li Z.Y. (2012). Large-scale land cover mapping with the integration of multi-source information based on the Dempster-Shafer theory. *International Journal of Geographical Information Science* **26**(1), 169–191.

Scipal K., Wagner W., Trommler M. and Naumann K. (2002). The global soil moisture archive 1992-2000 from ERS scatterometer data: first results, 1399–1401.

Shen W., Qin Z. and Lin Z. (2019). remote sensing A New Restoration Method for Radio Frequency Interference Effects on AMSR-2 over North America.

Shen X., Walker J.P., Ye N., Wu X., Boopathi N., Yeo I.-Y., Zhang L., Zhu L. (2021). Soil moisture retrieval depth of P- and L-band radiometry: predictions and observations. *IEEE Transactions on Geoscience and Remote Sensing* **59**, 6814–6822.

Shen X., Walker J.P., Ye N., Wu X., Brakhasi F., Boopathi N., Zhu L., Yeo I.-Y., Kim E., Kerr Y., Jackson T. (2022a). Impact of random and periodic surface roughness on P- and L-band radiometry. *Remote Sensing of Environment* **269**, 112825.

Shen X., Walker J.P., Ye N., Wu X., Brakhasi F., Boopathi N., Zhu L., Yeo I.-Y., Kim E., Kerr Y., Jackson T. (2022b). Evaluation of the tau-omega model over bare and wheat-covered flat and periodic soil surfaces at P- and L-band. *Remote Sensing of Environment* **273**, 112960.

Shen X., Walker J.P., Ye N., Wu X., Brakhasi F., Zhu L., Kim E., Kerr Y., Jackson T. (2023). Evaluation of the tau-omega model over a dense corn canopy at P- and L-Band. *IEEE Geoscience and Remote Sensing Letters* **20**, 2504605.

Song P., Zhang Y., Guo J., Shi J., Zhao T. and Tong B. (2022). A 1km daily surface soil moisture dataset of enhanced coverage under all-weather conditions over china in 2003–2019. *Earth System Science Data*.

Taylor C.M., M d.J.R.A., Françoise G.P.H.P. and A D.W. (2012). Afternoon rain more likely over drier soils. *Nature* **489**(7416).

Thomas J.J. and Ann Y.H. (2001). Soil moisture and TRMM microwave imager relationships in the Southern Great Plains 1999 (SGP99) experiment. *IEEE T. Geoscience and Remote Sensing* **39**.

Tian S., Renzullo L.J., van Dijk A.I.J.M., Tregoning P. and Walker J.P. (2019). Global joint assimilation of GRACE and SMOS for improved estimation of root-zone soil moisture and vegetation response, Hydrol. Earth Syst. Sci., **23**, 1067–1081.

Vine D.M.L., Lagerloef G.S.E., Colomb F.R., Yueh S. and Pellerano F.A. (2007). Aquarius: An Instrument to Monitor Sea Surface Salinity From Space. *IEEE T. Geoscience and Remote Sensing* **45**.

Shen W., Qin Z., Lin Z. (2019). A New Restoration Method for Radio Frequency Interference Effects on AMSR-2 over North America. *Remote Sensing*, **11**.

Wang L., Fang S., Pei Z., Wu D., Zhu Y. and Zhu W. (2022). Developing machine learning models with multisource inputs for improved land surface soil moisture in china. *Computers and Electronics in Agriculture* **192**, 106623.

Xi J.J., Wen J., Tian H. and Zhang T.T. (2014). Applicability evaluation of AMSR-E remote sensing soil moisture products in Qinghai-Tibet plateau. *Transactions of the Chinese Society of Agricultural Engineering* (Transactions of the CSAE) **30**(13), 194–202.

Yan C., Shen H., He W., Liu S. and Qin L. (2008). Study on the Smiulation Model of Soil Moisture with Multiple Regression Method. *Journal of Hubei University for Nationallities* (Natuaral Science Edition) **26**(3), 241–245.

Yuan W.P. and Zhou G.S. (2004). Theoratical Study and Reasearch Prosepect on Drought Indices. *ADVANCES IN EARTH SCIENCE* **19**(6), 982–991.